A HAZARD MAP OF DYNAMIC OBJECTS USING LIDAR MOBILE MAPPING

A. Schlichting [a], C. Brenner [a]

[a]Institute of Cartography and Geoinformatics, Leibniz Universität Hannover, Germany - (alexander.schlichting, claus.brenner)@ikg.uni-hannover.de

KEY WORDS: Mobile Mapping, LiDAR, Driver Assistance Systems, Self-Driving Cars, Segmentation, Classification, Maps

ABSTRACT:

One of the hardest problems for future self-driving cars is to predict hazardous situations which may lead to accidents. Especially, the behaviour of pedestrians and cyclists is hard to predict, since they have the ability to appear suddenly in the field of view and to change their state abruptly. Human drivers solve this problem typically by having a deeper understanding of the scene. Knowing that there are certain areas, e.g. bus stops where pedestrians frequently cross, they lower their speed and raise their attentiveness to be prepared for unexpected events. The technical equivalent of this is to provide a hazard map, which serves as a prior for self-driving cars, enabling them to adjust driving speed and processing thresholds.
In this paper, we present a method to derive such a hazard map using LiDAR mobile mapping. Pedestrians and cyclists are obtained from a sequence of point clouds by segmentation and classification. Their locations are then accumulated in a grid map, which serves as a ‘heat map’ for possibly hazardous situations. To demonstrate our approach, we generated a map using LiDAR mobile mapping, obtained by twelve measurement campaigns in Hanover (Germany). Our results show different outcomes for the city center, residential areas, busy roads and road junctions. While repeated mapping using mobile mapping systems will not be a scaleable approach for future deployment, our experiment shows the results which may be obtained in the future by cooperative mapping using the built-in sensors of future cars.

1. INTRODUCTION

1.1 General Instructions

According to the global status report on road safety by the World Health Organization (World Health Organization, 2013), road traffic injuries are the eighth leading cause of death. 1.24 million people die annually as a result of a road injury. 27% of the road deaths are pedestrians and cyclists. In low- and middle-income countries this number even goes up to a third of all fatalities. Nowadays, there is the vision that automated, self-driving cars will help to reach the goal of zero traffic accidents.
The observation of human behaviour in traffic contributes to the solution of this problem. Humans will perform much better if they act in a familiar environment, especially if they know it from their daily commute and have observed possibly hazardous situations at certain locations in the past. Hence, it is not only the static ‘background’ information, which helps them to master the current situation but also the knowledge of areas which are more risky than others due to regular local events, such as accidents or dangerous situations. Even though this knowledge is just a prior, it helps to reduce the risk of such situations. With regard to vehicles it means that they have to analyze their environment continuously. Sensors like laser scanners or cameras can map dynamic objects, namely pedestrians and cyclists, that occur in traffic scenes. The on-board computer interprets the data and stores the crucial information in a joint map of all vehicles in a certain region. In this paper, we call this map a hazard map. However, the benefit of this map is not only restricted to driver assistance systems. It can also be used in public transportation planning, like the determination of bus stops, where the knowledge of high pedestrian occurrence is very helpful.

We created an initial hazard map by using LiDAR data measured by a Mobile Mapping System. We chose a LiDAR system because of its high accuracy combined with a high spatial resolution. To collect a sufficient amount of data, we took 12 measurements drives of the same 13km trajectory in Hanover (Germany). The principle procedure is shown in Figure 1. In a first step we segmented free-standing objects of every measurement. We looked at the extent of these objects and removed those, whose width and height is not appropriate. In the next step, we used certain features describing the shape of the remaining objects for a pedestrian and cyclist classification. The objects were classified as pedestrians/cyclists by a Random Forest classifier and saved in a map. Overall we detected more than 10,000 pedestrians and cyclists. As a result, we generated a

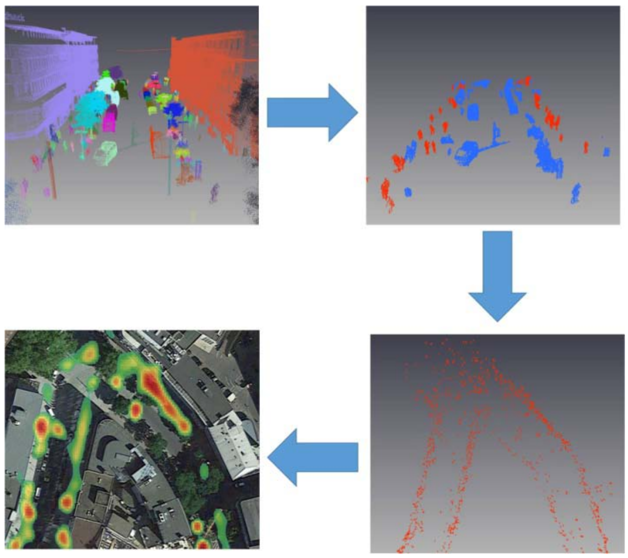

Figure 1: Steps of the hazard map generation: First, free-standing objects were segmented and classified as being pedestrians/cyclists or not. Next, classified dynamic objects of 12 measurement drives were aggregated and then saved in a map (Google Inc., 2015).

map where every cell indicates the probability of occurring pedestrians and cyclists.
Section 2 gives a review of related work. In section 3 the generation of the hazard map is described. The results of the pedestrian and cyclist detection are presented in section 4. Finally, in section 5 conclusions are drawn.

2. RELATED WORK

Pedestrian and cyclist detection plays an important role in driver assistance systems. In most cases image-based solutions are used, increasingly in combination with a stereo camera system. Oren et al. (Oren et al., 1997) use a wavelet template for pedestrian detection in mono camera images. Gavrilla (Gavrilla, 2000) uses a hierarchical template matching approach to detect pedestrians from moving vehicles with a reduced computation time. A stereo-based approach is used in Zhao and Thorpe (Zhao and Thorpe, 2000). Here, pedestrians are detected by neural networks in real-time. A more precise pedestrian detection method with regard to the position of the objects can be done by using LiDAR measurements. In Arras et al. (Arras et al., 2007) and Premebida et al. (Prembida et al., 2009) an automotive laser scanner with only one horizontal scan line is used to detect pedestrians. In both approaches the scanner measures the people's legs. Features are calculated and used to train a classifier and afterwards to classify the measured objects. In contrast, Spinello et al. (Spinello et al., 2010) use a 3D point cloud to detect pedestrians. The method divides the analyzed objects into several height cells, classifies each cell and then again joins the single cells. Although the pedestrian detection works for small distances, the accuracy decreases for longer ranges. The entire set of object points is analyzed in Navarro-Serment et al. (Navarro-Serment et al., 2010) and Kidono et al. (Kidono et al., 2011). Both calculate features describing the shape of the object. Next to statistical analyzes of every containing point, the main concept of Navarro-Serment et al. is to represent the 3D object as two 2D histograms, a main and a secondary plane. The amount of points in every histogram cell is used as a feature in a support vector machine (SVM) classifier. Kidono et al. additionally determine so called slice features to reduce the number of false positives. The slice features divide the point clusters into blocks with a specific height along the principal eigenvector. The object expansion along the two orthogonal eigenvectors is saved as a feature. In our pedestrian and cyclists classification approach, we mainly use features based on the classification concept of Navarro-Serment et al. (Navarro-Serment et al., 2010) and Kidono et al. (Kidono et al., 2011).
The generation of a map representing the probability of occurring pedestrians and cyclists has not been covered in literature so far. In Karimi (Karimi, 2012) the movement of pedestrians was simulated by an agent-based model. The goal in Orellana and Wachowicz (Orellana and Wachowicz, 2011) and Lerman et al. (Lerman, 2014) was to detect the movement behavior of pedestrians, especially places where people stop. In Orellana and Wachowicz GPS-modules were used to record the trajectory of pedestrians and to derive the movement vectors. In Lerman et al. pedestrians where counted by hand in different street segments and at different times. As a result a map of pedestrian movement was generated. In our approach we want to detect pedestrians and cyclists fully automatically and save them subsequently in a map.

3. GENERATION OF THE HAZARD MAP

The hazard map was generated by using Mobile Mapping data of 12 measurement campaigns in Hanover, Germany. For every point cloud pedestrians and cyclists are detected by an object segmentation and classification approach. The labelled pedestrians and cyclists are then registered in a map, realized as a 2D grid, where every cell indicates the probability of occurring dynamic objects.

Figure 2: Mobile Mapping System Riegl VMX-250 mounted on a van.

3.1 Data acquisition

The data was collected by a Riegl VMX-250 Mobile Mapping system, containing two Riegl VQ-250 laser scanners, a camera system and a localization unit. The system is shown in Figure 2.
The localization is provided by a highly accurate GNNS/INS system combined with an external Distance Measurement Instrument (DMI). The pre-processing step is made by the corresponding Riegl software and additional software for GNSS/INS processing, using reference data from the Satellite Positioning Service SAPOS. The resulting trajectory is within an accuracy of about 10 to 30 centimeters in height and 20 centimeters in position in urban areas.
Each scanner measures 100 scan lines per second with an overall scanning rate of 300,000 points per second (RIEGL, 2012). The measurement range is limited to 200 meters, the ranging accuracy is ten millimeters. Figure 3 shows a point

Figure 3: Point cloud gathered by the Mobile Mapping System

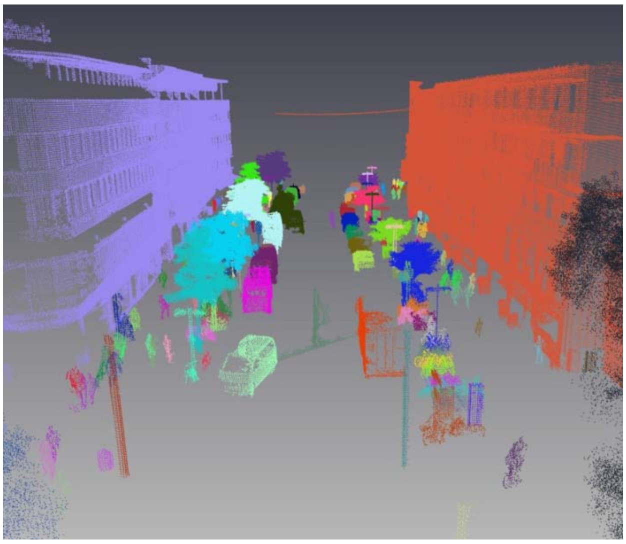

Figure 4: Segmented objects without ground

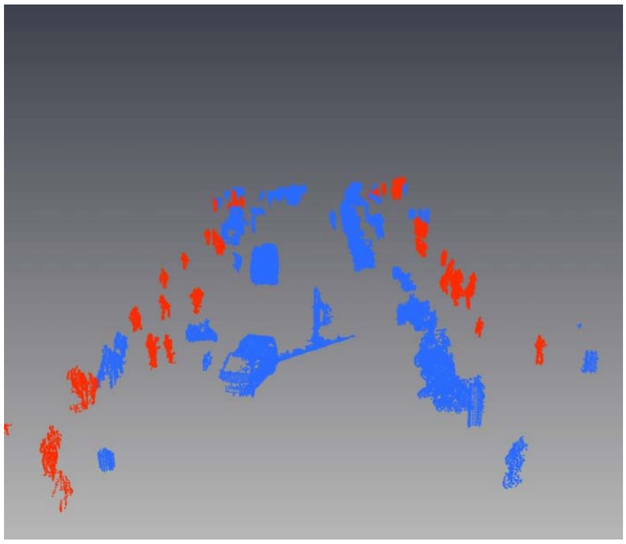

Figure 5: Classified objects with dynamic objects colored red.

cloud measured by the Mobile Mapping System, which is colored by the intensity of the reflected laser beam.

3.2 Pedestrian and cyclist detection

The pedestrian and cyclist detection consists of two steps. At first, we segment any free-standing objects from the point cloud, like pedestrians, cars, trees and buildings. Secondly, the segmented objects are classified. As we are only interested in pedestrians and cyclists, we can restrict the classification to two classes: pedestrians or cyclists and other objects. After the classification step the map's cells get updated for every detected pedestrian or cyclist.

The segmentation of free-standing objects is straightforward. If they are detached from the ground, the remaining points just have to be clustered. For both steps, the ground segmentation and the clustering step, we chose a seeded region growing approach, presented in Adams and Bischof (Adams and Bischof, 1994). First of all, the local normal vectors for every point using the 25 nearest neighbors are computed. In the next step, the seed points are picked from which the region starts to grow. As we want to segment the ground, we sort the points by their height and chose the k lowest points with a normal vector which points up within a tolerance of 0.2. Here k is given by 0.5 percent of the total number of points. For the growing step, a new point is added to the ground if it is within a radius of 20 centimeters and its local normal vector in z-direction points up within a certain tolerance. After every seed point has been processed, every point that belongs to a ground region is removed from the cloud. Next, a region growing is performed for the remaining points with only the Euclidean distance (20cm) as a growing threshold. The result is shown in Figure 4. As can be seen, pedestrians, poles, buildings, trees and cars were successfully separated from each other. Since we assume pedestrians and cyclists to have a specific maximum height, we additionally filter the objects by a height threshold of 2.5 meters.

Feature	Dimension
Object width	1
Object height	1
3D covariance matrix	6
Normalized 2D histogram for the main plane with 14 x 7 bins	98
Normalized 2D histogram for the secondary plane with 9 x 5 bins	45
Slice features	20

Table 1: Features for the pedestrian and cyclist classification.

The following step is the classification of the remaining objects which is done by the Random Forests implementation of the OpenCV library (Bradski, 2000). Random Forests are a set of decision trees and were introduced by Breiman in 2001 (Breimann, 2001). Prior to the classification step, training data has to be generated. The training data consists of objects with a known class label, whereby the objects are described by a feature vector. We used 2200 labeled objects to train the classifier: 500 pedestrians and cyclists and 1700 other objects. The feature vector has a size of 171 features, which are listed in table Table 1 and described in the following.

The first two features are the segment height and width. The next features are given by the 3x3 covariance matrix, which can be computed by performing a principal component analysis (PCA). First, the mean value in *x*/*y*/*z*-direction is subtracted from every segment point. The resulting points are then used to calculate the covariance matrix Σ by

$$\Sigma = \frac{1}{n-1} + \sum_{k=1}^{\infty n} (\mathrm{x_k} - \mathrm{m})(\mathrm{x_k} - \mathrm{m})^{\mathrm{T}} \qquad (1)$$

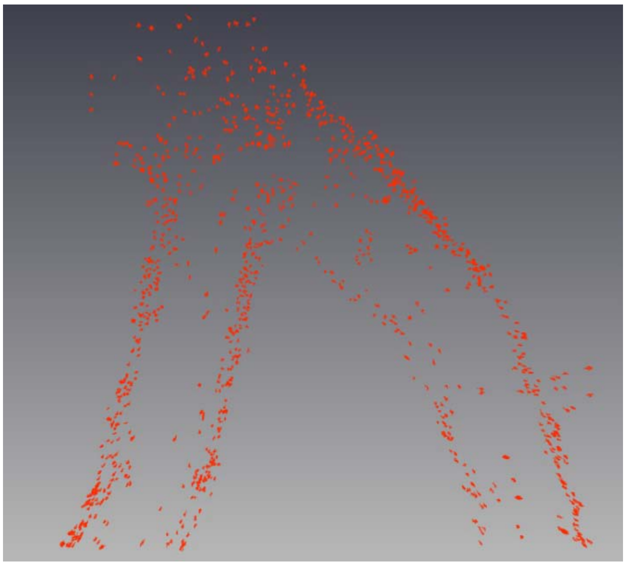

Figure 6: Classified dynamic objects of 12 measurement drives

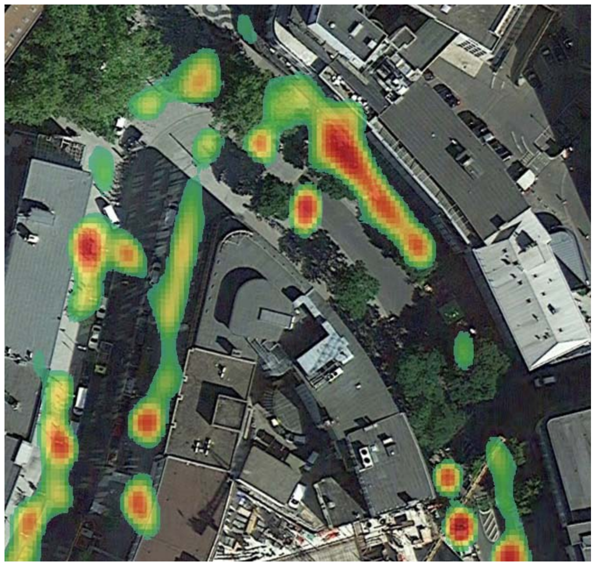

Figure 7: Dynamic map colored by cell values from green to red (Google Inc., 2015).

As Σ is a symmetric matrix, we only need to store six values in the feature vector. The remaining feature values are used to describe the shape of the objects by normalized 2D histograms. We divide the objects into a main and a secondary plane, as described in (Navarro-Serment et al., 2010). The main plane represents the front view of an object, the secondary plane the side view. Both planes are transferred into a normalized 2D histogram containing the number of points for every cell. Furthermore, we used so called slice features, introduced by (Kidono et al., 2011), to reduce false positive detections. The potential pedestrians and cyclists are divided into ten blocks of the same height along the *z*-direction. The block height depends on the overall object height. The features are then given by the point cluster width along the two horizontal eigenvectors of every block.
Finally, the trained Random Forest is used to classify every remaining object. Figure 5 shows the classified objects. Pedestrians and cyclists are colored red, other objects are colored blue.

3.3 Map generation

To generate the dynamic map, we created a grid of one meter cell length, where every object classified as pedestrian or cyclist is entered. We use a kernel density estimation approach, where every object increases the cell values in the surrounding, based on a normal distribution kernel. The standard deviation of the kernel is set to five meters. In addition, the cell values are weighted by their minimal distance to the road.

4. RESULTS

We used data from 12 measurement drives on four different days for the same 13km trajectory in Hanover (Germany) in a time slot from 07:00 to 18:00. Overall, we detected more than 10,000 pedestrians and cyclists. Figure 6 shows a crop of the detected objects. The resulting map can be seen in figureFigure 7. The whole map of the trajectory can be found in figure Figure 9 in the appendix. It can be seen that on road junctions and at central places the probability of occurring pedestrians is much higher than on large roads. In the city center, like in the northern streets in Figure 10, many hot spots occur, while on the road in the south of Figure 11, called *Friedrichswall*, the number of occurring pedestrians and cyclists is low.
The true positive rate of the Random Forest classification is 78.6%, the false negative rate 4.1%. In table Table 1 the result is compared to the respective false positive rate in Navarro-Serment et al. (Navarro-Serment et al., 2010) and Kidono et al. (Kidono et al., 2011). Although the chosen features are mostly similar, the classification performance in this approach is higher. One reason may be the high precision and point density of our Mobile Mapping data.

False negative classifications, meaning that a pedestrian or

(a) Typical pedestrian.

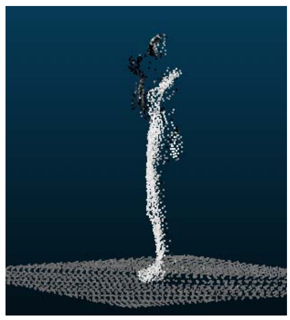

(b) Typical pedestrian (side view).

(c) Cyclist.

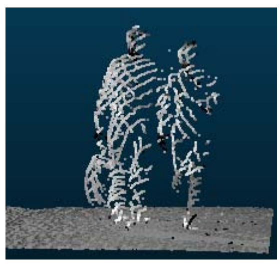

(d) Pedestrian pair.

Figure 8: Example point clusters of occurring pedestrians and cyclists.

cyclist was not detected as a dynamic object, mainly occur if the shape of the object is uncommon. In many cases the reason is that two people are walking close to each other, like shown in figure Figure 8(d). Typical pedestrian shapes like in figure Figure 8(a) and Figure 8(b) and also cyclists (figure Figure 8(c)) can be detected in general. We tried to improve the detection of pedestrian pairs by separating the pedestrian/cyclist-class into three classes: Pedestrians, cyclists and pedestrian pairs. This yielded to a worse classification performance with a joined true positive rate of only 62.6% and a slightly better false negative rate of 3.0% for the detection of dynamic objects. One solution for future works could be to separate a pedestrian pair into two single objects. Furthermore additional features, for example derived by the point reflection intensities, could be used to improve the classification.

Another problem are double detections of dynamic objects. Our Mobile Mapping System consists of two laser scanners, both measuring a vertical scan line. If e.g. a moving cyclist is registered by one scanner and a few moments later by the second scanner, the position of the dynamic object will have changed and it will appear two times in the point cloud. This problem may be solved by comparing dynamic objects to objects in their neighborhood and filter pedestrians and cyclists with a high correspondence. Alternatively, only one Scanner could be used, whereby this may yield to a worse classification performance and to dynamic objects, that are not captured by the Mobile Mapping System.

5. CONCLUSION

In this paper we presented a method to generate a map of dynamic objects, namely pedestrians and cyclists, fully automatically. We used a Mobile Mapping System to record LiDAR data in 12 measurement drives along a 13km trajectory in Hanover, Germany. Pedestrians and cyclists were detected in two steps: First, free-standing objects were segmented using a Region Growing algorithm. In the next step the objects were filtered and classified. A Random Forest implementation was used to classify the dynamic objects by the use of 171 features describing the shape of the individual objects. We achieved a true positive detection rate of 78.6% and a false negative rate of 4.1%. Overall we detected more than 10,000 pedestrians and cyclists. In future works, the detection rate can be increased by improving the object segmentation and using additional features.

In the next step the dynamic objects are accumulated in a 2D grid with a cell size of 1m. We call this grid hazard map. For every detected pedestrian and cyclist the appropriate cell value and its surrounding cell values get increased, dependent on the distance to the road. The generated map shows that in central places the occurrence of pedestrians and cyclists is much higher than on large roads.

Possible applications of hazard maps are driver assistance systems. Intelligent lighting systems can use the information gained by the map to illuminate hazardous areas where the probability of occurring dynamic objects is high. Automated vehicles also can adapt their driving behaviour in regions with a high probability. Though we call it a hazard map, it can also be used in other contexts. Smarter (public) traffic systems can be designed based on this map. Further the map could be used for location analyses of different kind of services and shops.

The map generation is so far based on point clouds which are currently captured with an expensive and highly accurate Mobile Mapping System. For the future, data can be collected using a crowd based approach, e.g. using mono/stereo cameras which anyhow will be built into most vehicles.

REFERENCES

Adams, R. and Bischof, L., 1994. Seeded region growing. Pattern Analysis and Machine Intelligence, IEEE Transactions on 16(6), pp. 641–647.

Arras, K. O., Mozos, O´ . M. and Burgard, W., 2007. Using boosted features for the detection of people in 2d range data. In: Robotics and Automation, 2007 IEEE International Conference on, IEEE, pp. 3402–3407.

Bradski, G., 2000. The OpenCV Library. Dr. Dobb's Journal of Software Tools.

Breiman, L., 2001. Random forests. Machine learning 45(1), pp. 5–32.

Gavrila, D. M., 2000. Pedestrian detection from a moving vehicle. In: Computer VisionłECCV 2000, Springer, pp. 37–49.

Google Inc., 2015. Google Maps, GeoBasis-DE/BKG. [Online]. Available from: http://www.google.de/maps/. [Accessed 1st October 2015].

Karimi, K., 2012. A configurational approach to analytical urban design:space syntaxmethodology. Urban Design International 17(4), pp. 297–318.

Kidono, K., Miyasaka, T., Watanabe, A., Naito, T. and Miura, J., 2011. Pedestrian recognition using high-definition lidar. In: Intelligent Vehicles Symposium (IV), 2011 IEEE, IEEE, pp. 405–410.

Lerman, Y., Rof`e, Y. and Omer, I., 2014. Using space syntax to model pedestrian movement in urban transportation planning. Geographical Analysis 46(4), pp. 392–410.

Navarro-Serment, L. E., Mertz, C. and Hebert, M., 2010. Pedestrian detection and tracking using three-dimensional ladar data. The International Journal of Robotics Research.

OpenStreetMap Foundation, 2015. OpenStreetMap. [Online]. Available from: https://www.openstreetmap.org/. [Accessed 1st October 2015].

Orellana, D. and Wachowicz, M., 2011. Exploring patterns of movement suspension in pedestrian mobility. Geographical analysis 43(3), pp. 241–260.

Oren, M., Papageorgiou, C., Sinha, P., Osuna, E. and Poggio, T., 1997. Pedestrian detection using wavelet templates. In: Computer Vision and Pattern Recognition, 1997. Proceedings., 1997 IEEE Computer Society Conference on, IEEE, pp. 193–199.

Premebida, C., Ludwig, O. and Nunes, U., 2009. Exploiting lidar-based features on pedestrian detection in urban scenarios. In: Intelligent Transportation Systems, 2009. ITSC'09. 12th International IEEE Conference on, IEEE, pp. 1–6.

RIEGL Laser Measurement Systems GmbH, 2012. RIEGL VMX-250. Technical report, RIEGL Laser Measurement Systems GmbH.

Spinello, L., Arras, K. O., Triebel, R. and Siegwart, R., 2010. A layered approach to people detection in 3d range data. In: AAAI. World Health Organization, 2013. Global status report on road safety. [Online]. Available from: http://www.who.int/violence_injury_prevention/road_safety_status/2013/report/en/. [Accessed 6th October 2015].

Zhao, L. and Thorpe, C. E., 2000. Stereo-and neural networkbased pedestrian detection. Intelligent Transportation Systems, IEEE Transactions on 1(3), pp. 148–154.

APPENDIX

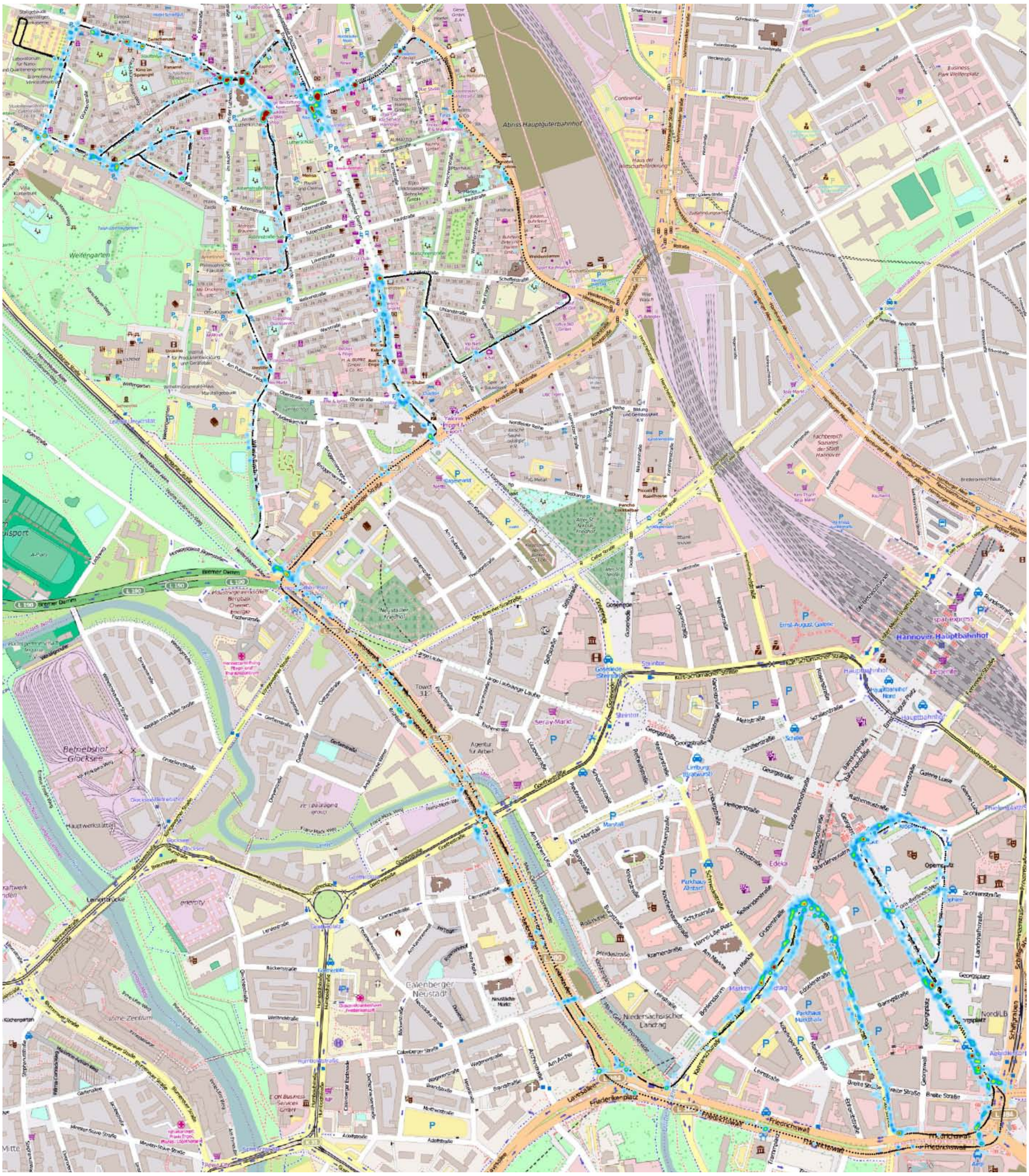

Figure 9: Map overview.

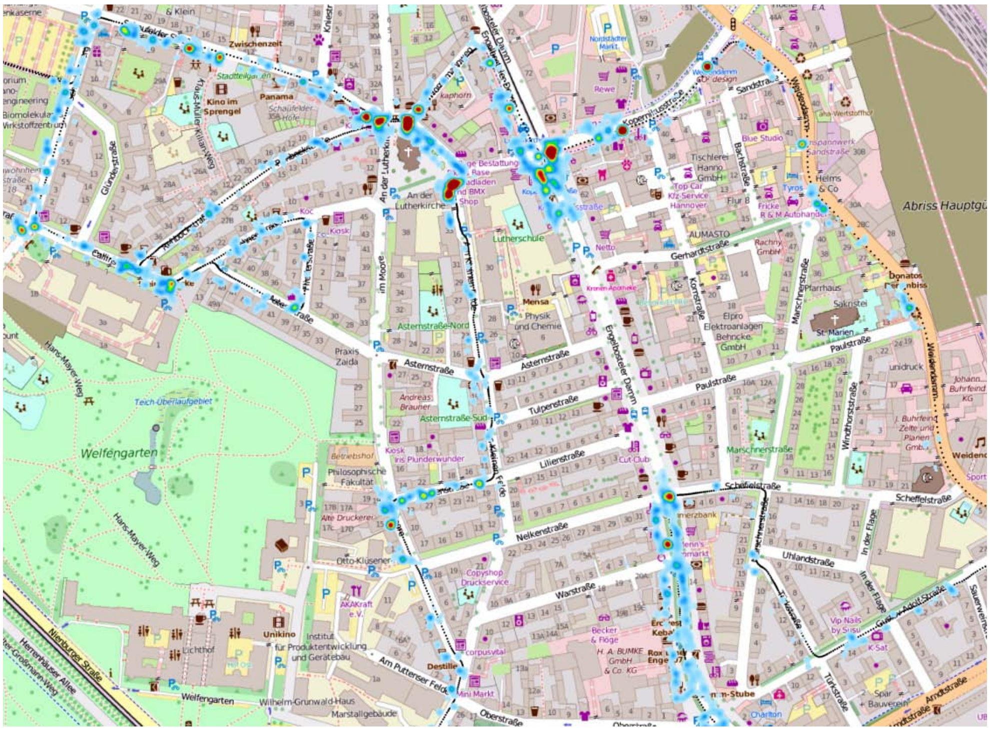

Figure 10: Northern part of the hazard map.

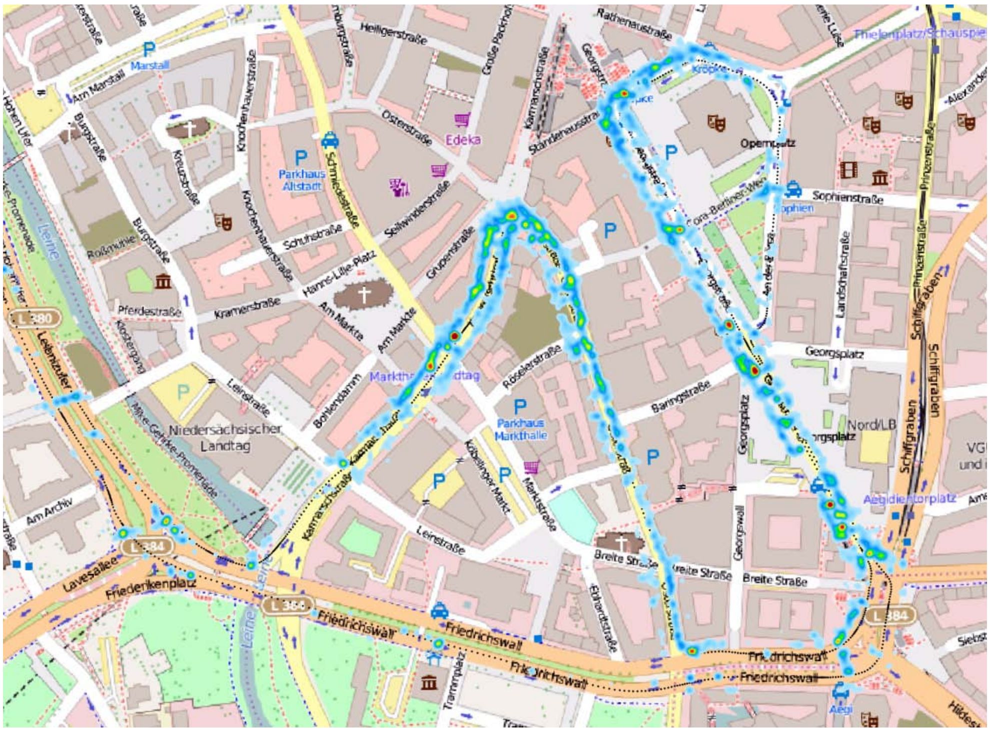

Figure 11: Southern part of the hazard map.